A Silica Bilayer Supported on Ru(0001): Following the Crystalline-to Vitreous Transformation in Real Time with Spectro-microscopy

Hagen W. Klemm, Mauricio J. Prieto,* Feng Xiong, Ghada B. Hassine, Markus Heyde, Dietrich Menzel, Marek Sierka,* Thomas Schmidt, and Hans-Joachim Freund

Abstract: The crystalline-to-vitreous phase transformation of a SiO₂ bilayer supported on Ru(0001) was studied by time-dependent LEED, local XPS, and DFT calculations. The silica bilayer system has parallels to 3D silica glass and can be used to understand the mechanism of the disorder transition. DFT simulations show that the formation of a Stone–Wales-type of defect follows a complex mechanism, where the two layers show decoupled behavior in terms of chemical bond rearrangements. The calculated activation energy of the rate-determining step for the formation of a Stone—Wales-type of defect (4.3 eV) agrees with the experimental value. Charge transfer between SiO₂ bilayer and Ru(0001) support lowers the activation energy for breaking the Si−O bond compared to the unsupported film. Pre-exponential factors obtained in UHV and in O₂ atmospheres differ significantly, suggesting that the interfacial ORu underneath the SiO₂ bilayer plays a role on how the disordering propagates within the film.

Introduction

The atomic scale processes and dynamics governing the glass transition are still questions that remain unresolved within the field of solid state theory[1] as well as experimentally.[2] However, over the last decades considerable progress has been made using the thin oxide film approach by allowing researchers to use traditional surface science methods in the characterization of well-defined oxide materials serving as model system. With this approach, fundamental questions can be tackled in a controlled and reproducible way. In this sense, the introduction of the silica system supported on Ru(0001) has made possible the preparation of monolayer (ML) and bilayer (BL) SiO₂ films. Even though in the case of the ML film the SiO₂ layer is chemically attached to the substrate, the SiO₂ BL presents itself as a self-contained film with all Si−O bonds saturated, and chemically detached from the Ru(0001) substrate, interacting with it only via dispersive forces.[3]

Particularly in the case of the silica BL supported on Ru(0001), two distinctive physisorbed SiO₂ BL films can be obtained, namely: crystalline[4] and vitreous.[5] Scanning tunneling microscopy (STM) revealed that in the case of crystalline bilayer films a well-defined structure is always found, consisting of SiO₄ corner-sharing tetrahedra creating hexagonal channels going all the way through the film down to the metallic support. As a consequence of the structure adopted, the crystalline BL shows a well-ordered arrangement of six-membered rings of alternating Si and O atoms, manifesting itself as a (2 × 2) structure in low-energy electron diffraction (LEED).[4] On the other hand, in the disordered state (vitreous), the surface structure of the bilayer changes exhibiting a rather broad distribution of ring sizes in comparison with the crystalline polymorph.[5] In the vitreous polymorph, ring sizes in the range of 4–9 members can be found without any disorder of the film in the direction normal to the surface,[6] where the existence of Si−O−Si bridges provides a good alignment of the two layers, thus preserving the pores that act as permeation channels for atoms/molecules. Interestingly, previous STM studies have reported that crystalline and vitreous forms of the bilayer can coexist giving a hint on how the disordering of the crystalline BL can proceed.[7] All the studies reported so far allowed us to verify in real space the hypothesis proposed by Zachariasen on the atomic arrangement in glass.[8] However, no direct information has been reported yet on the dynamics of the transformation or even how it can be controlled. Understanding how the transition between the two SiO₂ BL polymorphs occurs is of utterly importance and still a matter of debate. A

[*] Dr. H. W. Klemm, Dr. M. J. Prieto, Dr. M. Heyde, Dr. D. Menzel,
    Dr. T. Schmidt, Dr. H.-J. Freund
    Fritz-Haber Institute of the Max-Planck Society
    Faradayweg 4–6, 14195-Berlin (Germany)
    E-mail: prieto@fhi-berlin.mpg.de

    Dr. F. Xiong
    Department of Chemical Physics
    University of Science and Technology of China
    Hefei 230026 (P. R. China)

    G. B. Hassine, Dr. M. Sierka
    Otto-Schott-Institut für Materialforschung
    Friedrich-Schiller-Universität Jena
    Löbdergraben 32, 07743 Jena (Germany)
    E-mail: marek.sierka@uni-jena.de

    Dr. D. Menzel
    Physik-Department E20, Technical University München
    85748 Garching (Germany)

    Dr. F. Xiong
    Current address: Sinopec Shanghai Research Institute of
    Petrochemical Technology (SRIPT)
    Shanghai 201208 (China)

recent publication of a transmission electron microscopy (TEM) study has reported the experimental observation of the 5-7-5-7 to 6-6-6-6 ring system transformation in crystalline BL silica, with the process triggered by electron bombardment,[9] as opposed to the classical thermal activation. Nonetheless, it is believed that the phase transformation follows a path similar to the classical Stone–Wales mechanism,[10] as already described in the literature for a variety of materials such as graphene,[11] nanotubes,[12] and aromatic molecules.[13]

The mechanism of the order–disorder phase transformation in the silica bilayer is still the main question we address herein, applying a real-time approach using low-energy electron microscopy (LEEM) and LEED. This approach has proven to be a powerful technique in previous studies reporting different phase transformations in different materials.[14] In the present report we show that the phase transformation of a crystalline silica bilayer can be finely controlled by tuning the annealing temperature of the film during the film preparation procedure. Moreover, by following the temperature dependence of the rate at which the disorder process occurs, we obtain the apparent activation energy (E_a^{app}) for the crystalline-to-vitreous transformation of the SiO_2 BL on Ru(0001), thus providing some insight into the mechanism and the driving force of the process. Finally, based on DFT simulations we provide a detailed atomistic mechanism for the formation of a 5-7-5-7 Stone–Wales-type of defect starting from the perfectly hexagonal SiO_2 bilayer. Furthermore, charge density analysis is used to rationalize the influence of the metal support on the energetics of the transformation.

Results and Discussion

The atomic structure of both the crystalline and vitreous phases of SiO_2 bilayer was unveiled in the last decade by atomically resolved STM imaging.[7,15] Rigorous analysis has shown that the two-dimensional structure of the silica bilayer film in its crystalline and vitreous forms is well-defined as stated above and shown in Figure 1. However, it is important to mention that both polymorphs present characteristic LEED patterns, as shown in the inset of the Figure, thus allowing us to address directly both the crystallinity of the SiO_2 films and the dynamics of the transformation.

With the aim of quantitatively assessing the energetic aspects of the phase transformation, the time dependence of the intensity of the (0,0) LEED spot was analyzed at variable temperatures. An important aspect worth mentioning at this point is that the transformation can be triggered both in ultra-high vacuum (UHV) and in O_2 atmosphere, provided that the starting point is always the crystalline film. All measurements were performed at different temperatures starting always from a freshly prepared film. For the phase transformation performed in O_2 atmosphere, after the deposition of the corresponding amount of Si, the sample was annealed in 5×10^{-6} mbar O_2 at the temperature of interest (T_i) at which the LEED pattern was recorded with time. In this way, the typical behavior is the obtention of the crystalline SiO_2 BL in a first
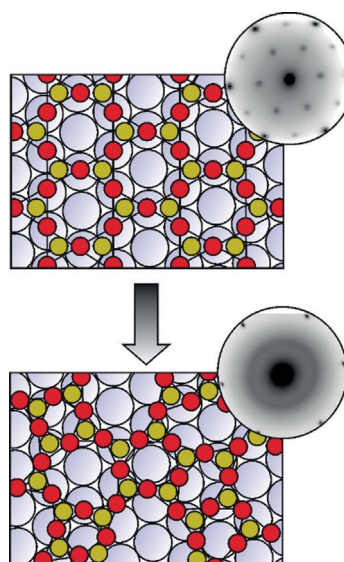

Figure 1. Models depicting the transformation of a crystalline (top) into a vitreous (bottom) SiO_2 bilayer on Ru(0001). O red, Si yellow spheres. Experimental LEED patterns are added to the corresponding structure.

step that converts into the vitreous BL after keeping T_i constant for some time.

However, in the case of the transformation triggered in UHV, an intermediate step needed to be introduced to guarantee the same starting point for the transformation as in oxygen atmosphere. Thus, in a first step a crystalline BL was produced by annealing the corresponding amount of Si in 5×10^{-6} mbar O_2 first at 1048 K. Once the crystalline film is obtained, the sample was cooled down and held at 775 K until the background pressure dropped below 5×10^{-9} mbar. Only then, the sample was rapidly annealed to the final transformation temperature T_i, as indicated. The time evolution of the (00) spot intensity at different temperatures and their fittings can be seen in Figure 2, for experiments performed in UHV and in O_2 atmosphere.

To determine the temperature dependence of the transformation rate, the time evolution of the (0,0) LEED spot intensity in both atmospheres (UHV and O_2) was analyzed. At the electron energy chosen for the real time experiments (42 eV) the electron reflectivity increases with time as the transformation to a disordered state (vitreous BL) progresses. The time-dependent measured total intensity $I_{total}(t)$ of the (0,0) spot can be described as a sum of the two contributions from crystalline I_{cryst} and amorphous I_{amorp} areas, whereas $p(t)$ is the time depending surface portion converted to vitreous structure:

$$I_{total}(t) = (1-p(t))I_{cryst} + p(t)I_{amorp} \tag{1}$$

where the values I_{cryst} and I_{amorp} can be experimentally derived from the initial non-converted and the final completely converted states, respectively. Equation (1) then yields:

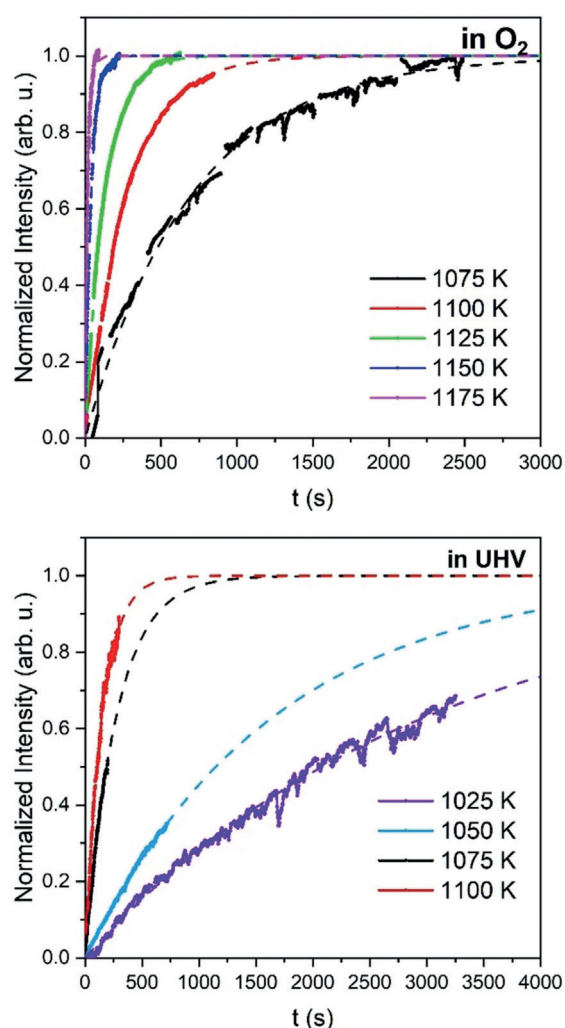$$p(t) = \frac{I_{total}(t)-I_{cryst}}{I_{amorp}-I_{cryst}} \tag{2}$$

Figure 2. Time evolution of the (0,0) LEED spot intensity collected at different temperatures, as color-labeled. Curves collected in 5×10^{-6} mbar O_2 and in UHV, as indicated. All dashed lines represent the results of the fittings for each curve.

The $p(t)$ curves obtained from Equation (2) are presented in Figure 2. With the aim of extracting the time constant for the different temperatures, each curve shown in Figure 2 was fitted with the following equation:

$$p(t) = 1 - e^{-\frac{t}{\tau}} \tag{3}$$

The conversion rate $R(t)$ is the derivative of $p(t)$ and gives in our case an exponential time dependent

$$R(t) = \frac{\partial}{\partial t} p(t) = \frac{1}{\tau} e^{-\frac{t}{\tau}} = \frac{1}{\tau}(1 - p(t)) \tag{4}$$

The values of the time constant τ extracted from the time dependent curves are presented in Table 1, with $1/\tau = R(t=0)$ representing the initial conversion rate. A series of LEED snapshots collected during the crystalline-to-vitreous transformation of the SiO_2 bilayer at high temperature is presented in the Supporting Information, Figure S1.

Table 1: Time-constant values resulting from the fitting of the time-dependent LEED intensity curves.[a]

T [K]	τ [s] (in UHV)	τ [s] (in O_2)
1175	–	16
1150	–	40
1125	–	128
1100	151	272
1075	274	692
1050	1657	–
1025	3000	–

[a] Curves are shown in Figure 2. Values correspond to the phase transformation performed in UHV and O_2 atmosphere.

Table 1 presents the time constant (τ) values obtained from the fitting procedure of curves and describing how fast the film is transformed. For more details on the procedure adopted, see the Supporting Information. The Arrhenius analysis in the form

$$\tau = \tau_0 \, e^{-(E_a^{app}/kT)}$$

of time constants τ is presented in Figure 3. From this analysis we obtain apparent activation energies for the crystalline-to-vitreous transformation of (4.2 ± 0.6) and (4.1 ± 0.2) eV, for the experiments performed in UHV and in O_2 atmosphere, respectively. From the experimentally determined E_a^{app} values it is possible to conclude that the presence of interfacial oxygen (O_{Ru}) does not play a role in the energetics of the phase transformation, since the values obtained are comparable within the uncertainty level. However, as seen from
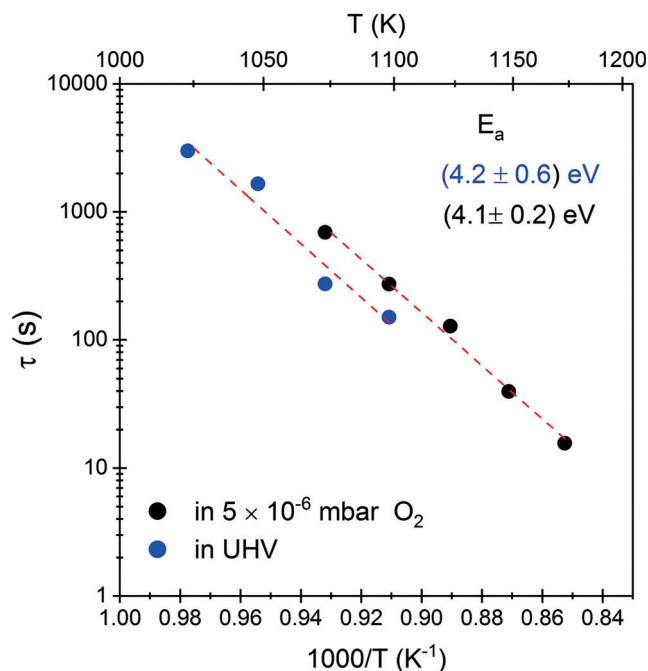

Figure 3. Arrhenius plot of the time constants extracted from the fitting measured at different temperatures in UHV and in O_2 atmosphere for a SiO_2 bilayer on Ru(0001).

Table 1, the disordering process of the silica bilayer takes a longer time when O_2 is present in the gas phase. In this sense, it is well known that the amount of O_{Ru} can be reduced under the silica bilayer, either by annealing in H_2 atmosphere at relatively mild conditions[16] or, like in the present case, just by annealing for extended periods of time in UHV conditions due to thermal desorption.[17] Since the temperatures at which the phase transformation was investigated in our experiments are above the onset for thermally induced desorption of O_2 (950 K),[18] the oxygen content under the silica bilayer is expected to be lower once the phase transformation is completed in the case of the UHV treatment, compared to the situation when O_2 is continuously dosed in the chamber during annealing. XPS spectra collected for two different vitreous SiO_2 BL produced in UHV and O_2 atmosphere are given in the Supporting Information, Figure S2. The O 1s spectra collected for both samples clearly show that the amount of interfacial oxygen is smaller for the film annealed in vacuum, thus confirming the thermal desorption of O_{Ru} at the temperatures used for annealing. Furthermore, both photoemission lines (Si 2p and O 1s) show a shift towards higher binding energies for the UHV annealed film, also consistent with the removal of O_{Ru} (that is, reduced interface dipole), as reported in previous publications.[16, 19]

In principle, the possibility of the silica bilayer to feel the electronic corrugation of the O/Ru(0001) would leave the energetic aspects of the phase transformation unmodified, provided that interactions between the substrate and the silica film are only weak dispersive forces. However, the registry between the silica film and the substrate lattice could affect the number of successive Stone–Wales processes in the atomic scale, thus affecting the transformation initial rates.

Since the vitreous bilayer silica film is characterized by a distribution of different ring sizes,[5] it is reasonable to assume that a number of consecutive rotations of the SiO_4 building units in the BL film may lead to its formation. Our observations suggest that the formation of the first Stone–Wales-type of defect is rate determining for the whole transformation process and, since the following rotations happen on a faster time scale, it seems likely that it is the formation of the first 5-7-5-7 ring configuration that act as nucleation points for the full transformation of the silica film into the vitreous form. It is important to point out that, under the experimental conditions used, no reversibility of the crystalline-to-vitreous transformation process was observed on the timescale of our experiments, without any indication neither in LEEM nor in LEED of big domains of coexisting phases. In this sense, the apparent irreversibility of transformation could be explained by the existence of a higher energy barrier for the reverse process (vitreous to crystalline). In this case, rising the temperature would allow to overcome the barrier for crystallization, but also increase the rate at which the vitreous phase is formed (initially with a lower E_a^{app}), thus making virtually impossible to achieve the crystalline state from the vitreous bilayer.

To understand the mechanism leading to the formation of a 5-7-5-7 structural element, DFT calculations were performed on a free-standing silica bilayer, with the aim of isolating substrate effects. Figure 4a shows a sequence of intermediate (I) and transition state (TS) structures for the proposed mechanism of the formation of a Stone–Wales-type of defect, starting from a perfect defect-free hexagonal silica bilayer. The proposed mechanism consists on the consecutive rotation of two contiguous SiO_4 units on one sheet of the bilayer, followed by the corresponding rotation of the SiO_4 units of the second sheet. Four elementary steps are identified, with a key intermediate (structure 2) containing a Stone–Wales-type of defect in only one of the hexagonal silica layers having an energy of 4.2 eV above that of the perfect bilayer with a 6-6-6-6 ring configuration. The energy of the final state 3 containing the 5-7-5-7 arrangement in both layers has an electronic energy 2.98 eV above that of the perfect silica bilayer (structure 1), with all transformation steps involving the concerted reconnection of Si–O bonds.

The potential energy diagram in Figure 4b summarizes the energetic aspects of the phase transformation. It is important to note at this point that the simultaneous rotation of four SiO_4 tetrahedral units on both planes of the bilayer is discarded based on the much higher E_a values obtained (ca. 25 eV). A movie is included in the Supporting Information that shows animation of the 6-6-6-6 to 5-7-5-7 transformation.

A detailed description of the transformation mechanism is as follows. The first step is breaking a Si–O bond within one of the silica sheets of the SiO_2 bilayer. The disconnected O atom resulting from this step reconnects to another Si atom constituting the first transition state (TS1) with an energy barrier of 6.13 eV and resulting in the formation of a single two-membered ring. Concomitantly, one of the Si–O bonds within the two-membered ring is broken and leads to the first intermediate structure (I1) with a Si-O dangling bond and a Si atom coordinated by three O atoms. This intermediate structure I1 lies 5.09 eV above the energy of the crystalline SiO_2 bilayer.

The following step corresponds to the formation of the intermediate structure 2, characterized by a complete 5–7-5-7 ring arrangement in one of the silica sheets of the bilayer, through the transition structure TS2 with an energy barrier of 3.57 eV. This structure contains one fully formed five-membered ring and one Si–O dangling bond. It is after the completion of this step that the transformation has been completed in half.

However, for the defect formation to be complete, the second layer must undergo similar processes as those already described to form the fully formed 5-7-5-7 defect, as depicted in Figure 4. Thus, for the second layer, two more transition states must be overcome with activation energies of 5.36 and 0.69 eV for the first and second steps, respectively, and the formation of the intermediate structure I3. It is important to mention that the values extracted from our calculations for the energy of formation of a Stone–Wales-type of defect (2.98 eV) is in good agreement with that reported by Björkman et al.[20] (2.8 eV) for the same type of structural element formed through a different mechanism. Furthermore, our mechanism is consistent with the description of 5-7-5-7 to 6-6-6-6 transformation triggered by electron bombardment, in which several metastable intermediate states were observed in the inverse process.[9]
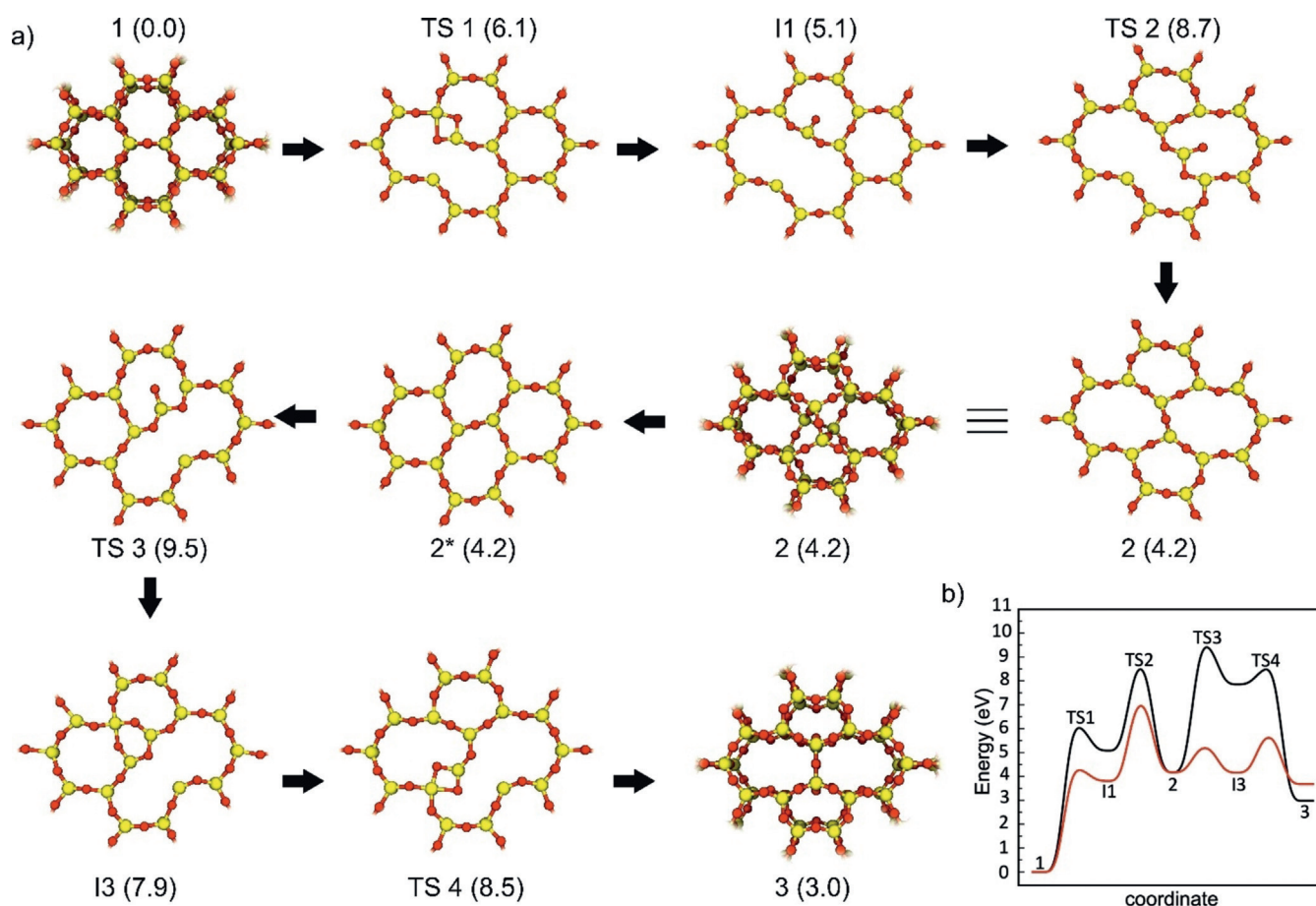
Figure 4. a) Intermediates and transition structures for the formation of a Stone–Wales defect in the first SiO₂ layer of a bilayer. All energies are in eV and related with that of structure 1 in parentheses (eV). 1, 2, and 3 show both silica layers in the bilayer arrangement. For the remaining structures only one silica layer is shown where the process takes place. Si yellow, O red. b) Potential energy diagram representing the transformation of a 6-6-6-6 into a 5-7-5-7 ring arrangement in a free-standing SiO₂ film (black) and a SiO₂ film supported on Ru(0001) (red). Note that all structures shown after structure 2* correspond to the opposite side of the SiO₂ BL shown in the first steps of the process.

According to our calculations the rate determining step for the formation of a Stone–Wales-type of defect in a free-standing silica bilayer is that from the initial structure 1 (perfect hexagonal arrangement) to intermediate structure I1, with an activation energy of 6.12 eV. This value is about 2 eV higher than those determined experimentally. Therefore, a study of SiO₂ BL supported on Ru(0001) was performed. The Stone–Wales-type of defect mechanism of SiO₂/Ru(0001) follows the same process as in the free-standing film presenting intermediate states in both silica layers. However, relative energies of the key intermediate and transition structures are significantly lowered compared to the free-standing film. In the presence of Ru(0001), the stability of all intermediate structures is similar and comparable to the final 5-7-5-7 structure, which is 3.7 eV above the perfect SiO₂ BL structure. The first, rate-determining step for the Stone–Wales transformation in SiO₂/Ru(0001) has an energy barrier of 4.3 eV, which is in very good agreement with the experimental values of 4.1–4.2 eV. It is worth mentioning at this point that the topmost layer of the silica film was proposed to be the starting place of the transformation under the assumption that for the bottom layer the same process would be energetically more demanding due to the interaction with the Ru substrate via dispersive forces.

The charge density analysis of SiO₂/Ru(0001) (see the Supporting Information) reveals a significant charge redistribution between the SiO₂ BL and the metal support along with a formation of interface dipole moments, in agreement with previous findings.[21] For the stable structures 1, 2, and 3 as well as I3, TS3, and TS4 between 0.6 and 0.7 electrons per surface unit cell are transferred from the SiO₂ BL to Ru(0001), leaving the BL slightly positively charged. However, in the case of the structures I1, TS1, and TS2 that contain a broken Si–O bond in the upper SiO₂ layer, the amount of charge transferred is only approximately 0.4 electrons per surface unit cell. In these structures a part of electron density is transferred back from Ru(0001) to the SiO₂ BL and localized at the undercoordinated Si and O atoms of the broken Si–O bond see the green area in the differences of charge density profiles of I1, TS1, and TS2 in the Supporting Information). This contributes to the stabilization of the structure and effectively lowers the activation barrier for breaking of the Si–O bond.

It is important to mention that we have investigated if the source of the differences between observed experimental and calculated values could be the periodic boundary conditions used in the modelling of the system. For this, larger supercells were tested (5×3, 6×4, and 7×5), giving the same values for the relative energies of the intermediate structures within a range of accuracy of 0.1 eV, thus ruling out this possibility (see comparison of values obtained in the Supporting Information, Table S1).

Finally, in our calculations a defect free silica bilayer is used as the starting point of the transformation process. However, there is experimental evidence that the real scenario is far more complex. For instance, it has been shown by STM measurements that a series of defects can be observed in the crystalline bilayer films supported on Ru-(0001), such us: 5-5-8 antiphase, 5-7 rotational, and 4-8 domain boundaries.[19] In this sense, our mechanism described above shows that processes starting from silica layers strained by preexisting defects have transition states with lower activation energies (see TS2, TS3, and TS4 in Figure 4b). Thus, it is reasonable to assume that the rate determining step for the transformation process, corresponding to the first Si—O bond rearrangement in the silica framework, will be equally affected by the existence of domain boundaries in the film, yielding a lower effective activation energy. Interestingly, results reported by Björkman et al.[20] regarding the assessment of strain dissipation within the silica film owing to the formation of a Stone–Wales defect show that an area corresponding to roughly 2000 SiO_2 unit cells is affected by compressive and/or tensile strain. These results strongly suggest that long range interactions between two neighboring defects cannot be discarded, in agreement with our previous assumption.

Conclusion

We have demonstrated that it is possible to finely tune the degree of crystallinity for a silica bilayer supported on Ru by changing the temperature of the last step of the preparation procedure. Temperature-dependent measurements allowed us to experimentally determine, for the first time to the best of our knowledge, the apparent activation energy for the crystalline-to-vitreous transformation process and the result is in very good agreement with the formation of a Stone–Wales-type of defect. DFT simulations show that the transformation process is far more complex than originally thought, involving separate subsequent changes on the different layers of the film rather than a concerted process. Charge transfer between the silica bilayer and the metal support was found to stabilize intermediate structures and to lower activation barriers for breaking the Si—O bond compared to the free-standing film.

Acknowledgements

Conflict of interest

The authors declare no conflict of interest.

[1] P. W. Anderson, *Proc. Natl. Acad. Sci. USA* **1995**, *92*, 6653–6654.

[2] A. C. Wright, *J. Non-Cryst. Solids* **1994**, *179*, 84–115.

[3] B. Yang, W. E. Kaden, X. Yu, J. A. Boscoboinik, Y. Martynova, L. Lichtenstein, M. Heyde, M. Sterrer, R. Wlodarczyk, M. Sierka, J. Sauer, S. Shaikhutdinov, H. J. Freund, *Phys. Chem. Chem. Phys.* **2012**, *14*, 11344–11351.

[4] D. Löffler, J. J. Uhlrich, M. Baron, B. Yang, X. Yu, L. Lichtenstein, L. Heinke, C. Büchner, M. Heyde, S. Shaikhutdinov, H.-J. Freund, R. Włodarczyk, M. Sierka, C. Sauer, *Phys. Rev. Lett.* **2010**, *105*, 146104.

[5] L. Lichtenstein, C. Büchner, B. Yang, S. Shaikhutdinov, M. Heyde, M. Sierka, R. Włodarczyk, J. Sauer, H.-J. Freund, *Angew. Chem. Int. Ed.* **2012**, *51*, 404–407; *Angew. Chem.* **2012**, *124*, 416–420.

[6] C. Büchner, L. Lichtenstein, M. Heyde, H.-J. Freund in *Noncontact Atomic Force Microscopy, Vol. 3* (Eds.: S. Morita, F. J. Giessibl, E. Meyer, R. Wiesendanger), Springer International Publishing, Cham, **2015**, pp. 327–353.

[7] M. Heyde, S. Shaikhutdinov, H. J. Freund, *Chem. Phys. Lett.* **2012**, *550*, 1–7.

[8] W. H. Zachariasen, *J. Am. Chem. Soc.* **1932**, *54*, 3841–3851.

[9] P. Y. Huang, S. Kurasch, J. S. Alden, A. Shekhawat, A. A. Alemi, P. L. McEuen, J. P. Sethna, U. Kaiser, D. A. Muller, *Science* **2013**, *342*, 224–227.

[10] A. J. Stone, D. J. Wales, *Chem. Phys. Lett.* **1986**, *128*, 501–503.

[11] J. Ma, D. Alfè, A. Michaelides, E. Wang, *Phys. Rev. B* **2009**, *80*, 033407.

[12] L. G. Zhou, S.-Q. Shi, *Appl. Phys. Lett.* **2003**, *83*, 1222–1224.

[13] E. Brayfindley, E. E. Irace, C. Castro, W. L. Karney, *J. Org. Chem.* **2015**, *80*, 3825–3831.

[14] See, for example: a) E. Bauer, *Rep. Prog. Phys.* **1994**, *57*, 895; b) J. B. Hannon, R. M. Tromp, *Annu. Rev. Mater. Res.* **2003**, *33*, 263–288.

[15] C. Büchner, L. Lichtenstein, X. Yu, A. J. Boscoboinik, B. Yang, W. E. Kaden, M. Heyde, S. Shaikhutdinov, R. Włodarczyk, M. Sierka, J. Sauer, H. J. Freund, *Chem. Eur. J.* **2014**, *20*, 9176–9183.

[16] M. J. Prieto, H. W. Klemm, F. Xiong, D. M. Gottlob, D. Menzel, T. Schmidt, H.-J. Freund, *Angew. Chem. Int. Ed.* **2018**, *57*, 8749–8753; *Angew. Chem.* **2018**, *130*, 8885–8889.

[17] R. Włodarczyk, M. Sierka, J. Sauer, D. Löffler, J. J. Uhlrich, X. Yu, B. Yang, I. M. N. Groot, S. Shaikhutdinov, H. J. Freund, *Phys. Rev. B* **2012**, *85*, 085403.

[18] L. Surnev, G. Rangelov, G. Bliznakov, *Surf. Sci.* **1985**, *159*, 299–310.

[19] K. M. Burson, C. Büchner, M. Heyde, H. F. Freund, *J. Phys. Condens. Matter* **2017**, *29*, 035002.

[20] T. Björkman, S. Kurasch, O. Lehtinen, J. Kotakoski, O. V. Yazyev, A. Srivastava, V. Skakalova, J. H. Smet, U. Kaiser, A. V. Krasheninnikov, *Sci. Rep.* **2013**, *3*, 3482.

[21] M. Wang, J. Q. Zhong, J. Kestell, I. Waluyo, D. J. Stacchiola, J. A. Boscoboinik, D. Lu, *Top. Catal.* **2017**, *60*, 481–491.